

LETTER TO THE EDITOR

# Spatially-resolved Spectroscopic Analysis of Ly $\alpha$ Haloes

## Radial Evolution of the Ly $\alpha$ Line Profile out to 60 kpc

Yucheng Guo<sup>1\*</sup>, Roland Bacon<sup>1</sup>, Lutz Wisotzki<sup>2</sup>, Thibault Garel<sup>3</sup>, Jérémy Blaizot<sup>1</sup>, Joop Schaye<sup>4</sup>, Jorjy Matthee<sup>5</sup>,  
Floriane Leclercq<sup>6</sup>, Leindert Boogaard<sup>7</sup>, Johan Richard<sup>1</sup>, Anne Verhamme<sup>8</sup>, Jarle Brinchmann<sup>4,9,10</sup>, Léo  
Michel-Dansac<sup>1</sup>, and Haruka Kusakabe<sup>11</sup>

- <sup>1</sup> Univ Lyon, Univ Lyon1, Ens de Lyon, CNRS, Centre de Recherche Astrophysique de Lyon UMR5574, F-69230, Saint-Genis-Laval, France  
<sup>2</sup> Leibniz-Institut für Astrophysik Potsdam (AIP), An der Sternwarte 16, 14482 Potsdam, Germany  
<sup>3</sup> Observatoire de Genève, Université de Genève, 51 Ch. des Maillettes, 1290 Versoix, Switzerland  
<sup>4</sup> Leiden Observatory, Leiden University, P.O. Box 9513, 2300 RA Leiden, The Netherlands  
<sup>5</sup> Department of Physics, ETH Zürich, Wolfgang-Pauli-Strasse 27, 8093 Zürich, Switzerland  
<sup>6</sup> Department of Astronomy, University of Texas at Austin, 2515 Speedway, Austin, TX 78712, USA  
<sup>7</sup> Max Planck Institute for Astronomy, Königstuhl 17, 69117, Heidelberg, Germany  
<sup>8</sup> Observatoire de Genève, Université de Genève, Ch. Pegasi 51, CH-1290 Versoix, Switzerland  
<sup>9</sup> Instituto de Astrofísica e Ciências do Espaço, Universidade do Porto, CAUP, Rua das Estrelas, PT4150-762 Porto, Portugal  
<sup>10</sup> Departamento de Física e Astronomia, Faculdade de Ciências, Universidade do Porto, Rua do Campo Alegre 687, PT4169-007 Porto, Portugal  
<sup>11</sup> National Astronomical Observatory of Japan (NAOJ), 2-21-1, Osawa, Mitaka, Tokyo, 181-8588, Japan

Submitted 2023

### ABSTRACT

Deep MUSE observations have unveiled pervasive Ly $\alpha$  haloes (LAHs) surrounding high-redshift star-forming galaxies. However, the origin of the extended Ly $\alpha$  emission is still a subject of debate. We analyse the average spatial extent and spectral variation of the circumgalactic LAHs by stacking a sample of 155 Ly $\alpha$  emitters (LAEs) at redshift  $3 < z < 4$  in the MUSE Extremely Deep Field (MXDF). With respect to the Ly $\alpha$  red peak of the target LAE, the Ly $\alpha$  line peak becomes increasingly more blueshifted out to a projected distance of at least 60 kpc, where the velocity offset is  $\approx 250$  km/s. This signal is observed in both the mean and median stacks, and is thus a generic property of the LAE sample with typical Ly $\alpha$  luminosity  $\approx 10^{41.1}$  erg s<sup>-1</sup>. We discuss multiple scenarios to explain the blueshift of the circumgalactic Ly $\alpha$  line. The most plausible one is a combination of outflows and inflows. In the inner region of the LAH, the Ly $\alpha$  photons are produced by the central star formation and then scattered within outflows. At larger radii, the infalling cool gas shapes the observed Ly $\alpha$  blueshift.

**Key words.** galaxies: high-redshift – galaxies: formation – galaxies: evolution – intergalactic medium – cosmology: observations

## 1. Introduction

During the past decades, large samples of Ly $\alpha$  emitters (LAEs) have been efficiently identified in deep narrow band (NB) imaging and IFU observations (e.g. Ouchi et al. 2008; Shibuya et al. 2012; Guo et al. 2020; Ono et al. 2021; Richard et al. 2021; Bacon et al. 2023; Kikuta et al. 2023; Mentuch Cooper et al. 2023). Around the LAEs, extended Ly $\alpha$  emission, known as Ly $\alpha$  haloes (LAHs) are detected individually (e.g. Wisotzki et al. 2016; Leclercq et al. 2017) and through stacking (e.g. Momose et al. 2014; Wisotzki et al. 2018). We now know that the star-forming galaxies are typically surrounded by LAHs that are observed to be several to tens of times larger than the stellar continuum, indicating the presence of a significant amount of neutral hydrogen in the circumgalactic gas (e.g. Steidel et al. 2011; Ouchi et al. 2020; Kusakabe et al. 2022). Recent deep observations and stacking analyses have detected extended Ly $\alpha$  emission around LAEs out to hundreds of kpc, achieving a surface

brightness level of  $\approx 10^{-20}$  erg s<sup>-1</sup> cm<sup>-2</sup> arcsec<sup>-2</sup> (e.g. Kikuchi-hara et al. 2022; Lujan Niemeyer et al. 2022).

Despite the progress on mapping the surface brightness of the Ly $\alpha$  emission, its spectral variation is still poorly constrained. Spatially resolved spectroscopic studies of LAHs have so far mostly been performed using deep MUSE or KCWI observations on a small number of individual bright LAHs (e.g. Erb et al. 2018, 2023; Claeysens et al. 2019; Leclercq et al. 2020). Restricted by the S/N, these previous observations only focus on small distances from the central galaxy. The LAHs exhibit spatial variation of the Ly $\alpha$  line profiles within the inner  $\approx 20$  kpc (e.g. Claeysens et al. 2019; Leclercq et al. 2020), indicating variations in the column density, covering fraction or kinematics of the gas. Claeysens et al. (2019) found a trend that the peak of the Ly $\alpha$  line is shifted to redder wavelengths at large radii ( $\approx 20$  kpc), and that there is a strong correlation between the peak velocity shift and line width. Such a trend was also observed by Leclercq et al. (2020), in agreement with models of Ly $\alpha$  resonant scattering in outflows. Erb et al. (2018) performed a single case study with KCWI. They found higher blue-to-red

\* e-mail: yucheng.guo@univ-lyon1.fr

peak ratios and narrower separations of the two peaks at larger radii ( $\lesssim 30$  kpc). Erb et al. (2023) analyzed a sample of 12 double peaked LAEs. They found similar trends for peak ratios and separations as Erb et al. (2018). The MUSE stacking analysis of Gallego et al. (2021) discovered that the peak of the Ly $\alpha$  emission is blueshifted at large radii with respect to the central galaxy's Ly $\alpha$  line, though with large variation. Despite these observations, a comprehensive understanding of the spectral variations of LAHs as a collective population remains elusive, especially for the faint LAHs.

In this work, we use the the deepest MUSE dataset to measure Ly $\alpha$  spectral variation within LAHs. Through data stacking we study the generic spectral properties of the  $3 < z < 4$  LAE population out to large radial distances. In our previous work (Guo et al. 2023, hereafter Paper I), we measured the median Ly $\alpha$  surface brightness profiles out to 270 kpc. In this paper, we focus on the Ly $\alpha$  spectral profiles within 60 kpc, where the S/N is high enough for spectral analysis. We adopt the standard  $\Lambda$ CDM cosmology with  $H_0 = 70 \text{ km s}^{-1} \text{ Mpc}^{-1}$ ,  $\Omega_m = 0.3$  and  $\Omega_\Lambda = 0.7$ . All distances are proper, unless noted otherwise.

## 2. Data description and analysis

The MUSE eXtremely Deep Field (MXDF, Bacon et al. 2023) has a field of view of  $1'$  in diameter, with the longest exposure time of approximately 140 hours, and shortest exposure time of several hours. The MXDF is the deepest spectroscopic survey ever performed, reaching an unresolved emission line median  $1\sigma$  surface brightness limit of  $< 10^{-19} \text{ erg s}^{-1} \text{ cm}^{-2} \text{ arcsec}^{-2}$ . The MXDF survey enables studies of extremely low surface brightness emission, such as the detection of a cosmic web in Ly $\alpha$  emission on scales of several cMpc (Bacon et al. 2021). The survey design, sky coverage and data reduction of the MXDF are described in Bacon et al. (2023). Bacon et al. (2023) also provide the redshifts, multi-band photometry, morphological and spectral properties, as well as measurements of the stellar mass and star formation rate of all the galaxies discovered by the deep MUSE observations in the Hubble Ultra Deep Field (HUDF).

In total 420 LAEs have been detected in the MXDF. In this study, we focus on LAEs in the redshift range  $3 < z < 4$ , where the cosmological surface brightness dimming is relatively weak, the efficiency of MUSE is high, and there is no strong atmospheric OH emission. There are 155 LAEs in this redshift range. The median Ly $\alpha$  luminosity ( $L_{\text{Ly}\alpha}$ ) of these LAEs is approximately  $10^{41.1} \text{ erg s}^{-1}$ . The median stellar mass ( $M_*$ ) is approximately  $10^{7.6} M_\odot$ . More details of this LAE sample are presented in Bacon et al. (2023) and Paper I. In Paper I we estimate the typical virial radius ( $r_{\text{vir}}$ ) of this LAE sample based on the  $r_{\text{vir}}$  - UV magnitude relation predicted by the semi-analytic model of Garel et al. (2015). The typical virial radius  $r_{\text{vir}}$  of the sample is approximately 20 kpc.

We produce a  $21'' \times 21''$  MUSE mini-dataset centered on each LAE. We mask all the area with exposure time less than 110 hours in order to achieve a high S/N. We remove the continuum by performing spectral median filtering using a wide spectral window of 200 Å. We also mask all the emission and absorption lines from neighboring objects, based on the line catalogue and segmentation maps provided by Bacon et al. (2023).

In order to study the average spatially-resolved spectra of the LAHs, we adopt a full 3D stacking procedure. We shift individual mini-datasets and re-bin them to a common (rest-frame) wavelength frame based on the peak wavelength of the Ly $\alpha$  line. For LAEs with double peak Ly $\alpha$  lines, we use the wavelength

of the red peak. We produce the stacked datacubes in both mean and median.

## 3. Results

In Figure 1 we present the Ly $\alpha$  pseudo-NBs in a series of velocity bins of 200 km/s, with the full velocity coverage from -700 km/s to 700 km/s. These Ly $\alpha$  maps are extracted from the median-stacked datacube. The width of the pseudo-NBs (200 km/s) corresponds to approximately  $0.8 \text{ Å}$  at rest frame, and about 2-4 wavelength layers in the original MUSE datacubes. The middle velocity bin is centered on the Ly $\alpha$  line peak of the central galaxy. To improve the visualization of large-scale features, we spatially smoothed the NBs with a Gaussian filter with a FWHM of  $2.3''$ .

In Figure 1 we clearly see that the Ly $\alpha$  emission extends to several tens of kpc. The most extended Ly $\alpha$  emission does not reside at the peak of Ly $\alpha$  line, but is located at the velocity range of [-300 km/s, -100 km/s]. This suggests that at large radii the extended Ly $\alpha$  emission is bluer.

To confirm this blueshift trend of the extended Ly $\alpha$  emission (with respect to the Ly $\alpha$  red peak of the central galaxy), we measure the azimuthally averaged profiles of the Ly $\alpha$  line. The stacked spectra are shown in Figure 2. Different rows shows different radial distances. In both mean (left) and median (right), the Ly $\alpha$  line shifts from approximately 0 km/s in the center to approximately -250 km/s at  $\approx 60$  kpc. In the largest radial bin (29-59 kpc), the peak S/N of the Ly $\alpha$  line is  $\approx 3.2$ , and the accumulated S/N is  $\approx 7.2$ .

When we discuss the velocity shift, we must take into account the spectral resolution of MUSE, which is approximately 150 km/s at  $3 < z < 4$ , smaller than the measured Ly $\alpha$  line shift. While the low spectral resolution may increase the measurement uncertainty of the wavelength, it cannot produce the smooth trend of Ly $\alpha$  blueshift we see from 0 kpc to 60 kpc.

Bacon et al. (2023) provide the measurement errors for the Ly $\alpha$  peak wavelength. The median value of this error over the LAE sample is approximately 165.1 km/s. When considering the average over 155 LAEs, the stacked error should be approximately 14 km/s, which is evidently smaller than the velocity shift observed for the largest radial bin.

To ensure that the stacking is not dominated by a few outliers, we perform the following analysis. We randomly remove 15% of objects in the sample, and repeat the data stacking procedure. This process is iterated 100 times, and for each stack, we measure the Ly $\alpha$  peak velocity at 29-59 kpc. The resulting median velocity and its standard error are approximately -259 km/s and 18 km/s, respectively.

In summary, we detect a  $\approx 250$  km/s blueshift of the Ly $\alpha$  line (compared to the Ly $\alpha$  red peak of the central galaxy) from the galaxy out to 60 kpc ( $3 r_{\text{vir}}$ ). This blueshift trend is clearly observed in both mean and median stacks, and is not dominated by a few outliers. Hence, it is a common phenomenon for LAEs with Ly $\alpha$  luminosity  $10^{41.1} \text{ erg s}^{-1}$ .

Here we would like to point out that our observation provides important guidance for IFU data analyses. At large distances (tens of kpc), the bulk of the Ly $\alpha$  emission is bluer than the central Ly $\alpha$  red peak. Previous studies tended to apply a very narrow pseudo NB centered on the peak of Ly $\alpha$  line to enhance the S/N, which, however, loses the blue-shifted signal. In Paper I, we measure the Ly $\alpha$  surface brightness profile by reasonably wide pseudo-NBs (with width of 920 km/s at  $z = 3$ ), thus including the majority of the extended Ly $\alpha$  emission.

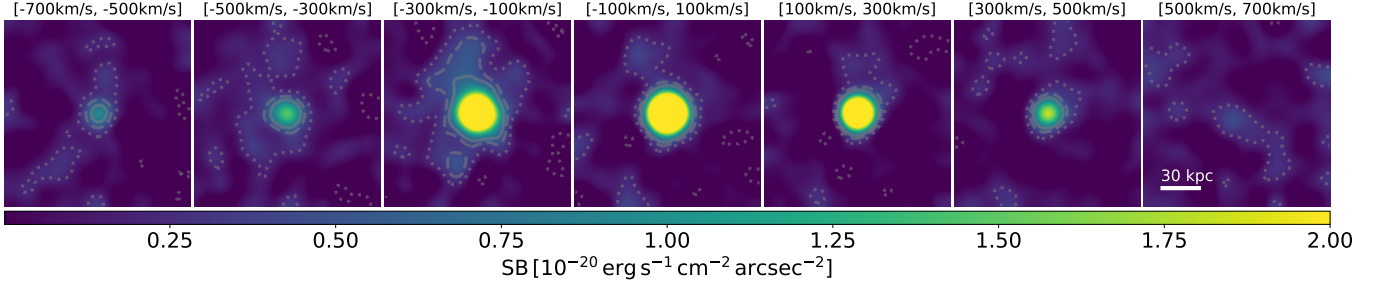


**Fig. 1.** Surface brightness maps of the median-stacked Ly $\alpha$  emission. Each panel shows the Ly $\alpha$  pseudo-NB in a velocity interval of 200 km/s. The zero point corresponds to the peak of the Ly $\alpha$  line. The NBs have been smoothed using a Gaussian kernel of width of 2.3". The grey contours correspond to Ly $\alpha$  significance levels of 2, 4 and 6  $\sigma$  (dotted, dashed and solid, respectively).

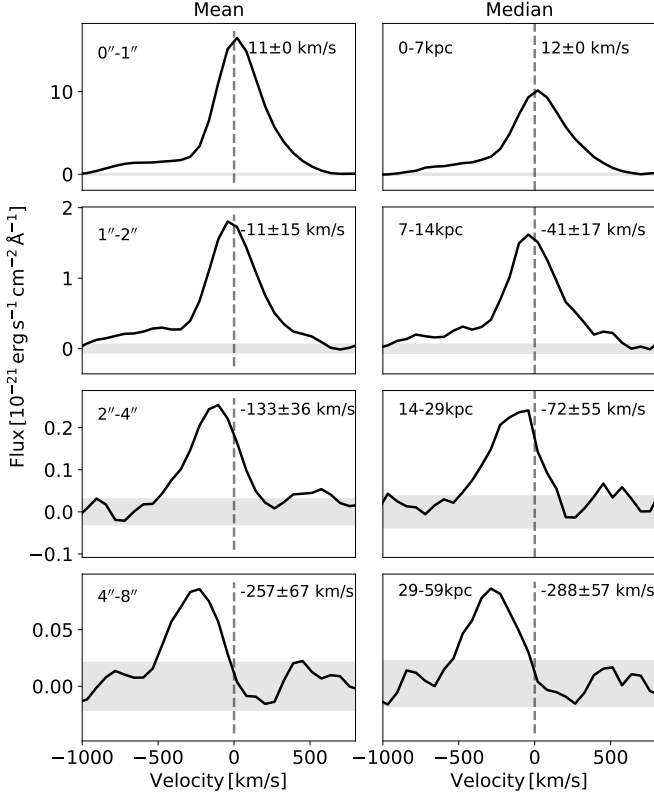


**Fig. 2.** Ly $\alpha$  line profiles at different distances from the central galaxy. The spectra in the left and right columns are derived from the mean- and median-stacked datacubes. Different rows show different radial bins ranging from 1" (7 kpc) to 8" (59 kpc). The vertical dashed lines denote the peak of the central Ly $\alpha$  line. The horizontal grey shaded regions show the 1 $\sigma$  error range.

### 3.1. The systemic redshift

In our previous analysis, we used the Ly $\alpha$  peak redshift ( $z_{\text{Ly}\alpha}$ ) as reference for spectral re-alignment and data stacking. Due to the resonant scattering of Ly $\alpha$  photons in the interstellar medium, the Ly $\alpha$  line usually deviates from the systemic redshift ( $z_{\text{sys}}$ , e.g. McLinden et al. 2011; Shibuya et al. 2014; Muzahid et al. 2020).

We utilize the estimated  $z_{\text{sys}}$  provided by Bacon et al. (2023) as the reference systemic redshift. This estimation is based on the empirical relation established by Verhamme et al. (2018). Then we repeat the data analysis of Section 2. The Ly $\alpha$  spectra in different radial bins are shown in Figure 3. In the inner  $\approx 10$  kpc, Ly $\alpha$  is redshifted by about 170 km/s relative to  $z_{\text{sys}}$ .

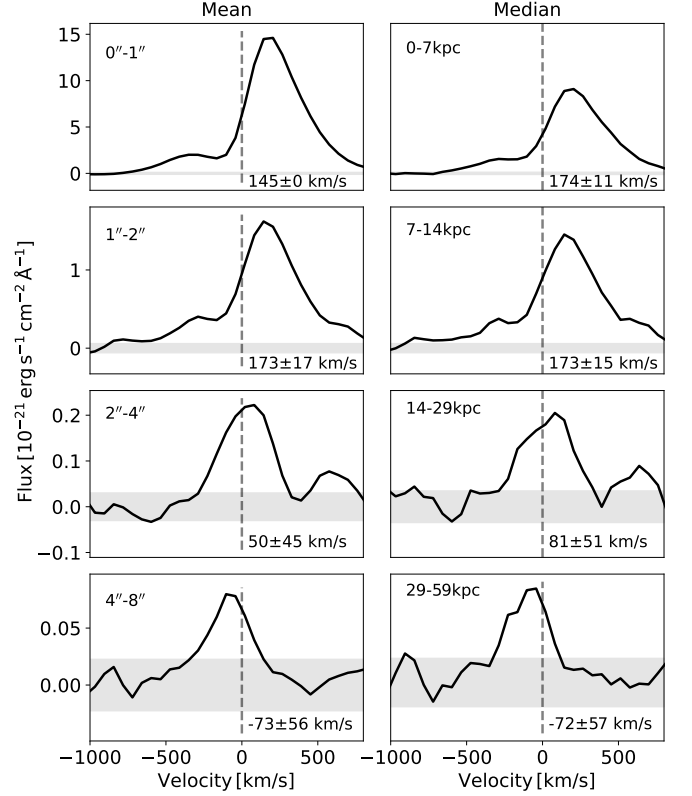


**Fig. 3.** As Figure 2, except that here all the mini-datacubes are re-aligned by the estimated  $z_{\text{sys}}$  instead of  $z_{\text{Ly}\alpha}$ .

With increasing distance, the Ly $\alpha$  line shifts to shorter wavelengths. For the final radial bin (29-59 kpc), the peak of the Ly $\alpha$  line is slightly bluer than  $z_{\text{sys}}$ , with a value of  $\approx -70$  km/s. This trend is seen in both mean and median stacks. The scatter of the  $z_{\text{sys}}$  estimation of Verhamme et al. (2018) is about 72 km/s. For a stack of 155 LAEs, the final error attributed to the  $z_{\text{sys}}$  estimation should be only a few km/s. However, due to the noise level and spectral resolution, it is difficult to better quantify the Ly $\alpha$  peak velocity in the final radial bin.

## 4. Discussion

Several physical mechanisms have been proposed to explain the production and propagation of Ly $\alpha$  photons in LAHs. Their relative importance may vary with radial distance (e.g. Mitchell et al. 2021; Byrohl et al. 2021). Here we explore several speculative considerations concerning the underlying physics responsi-

ble for the observed spectral shift of the Ly $\alpha$  line out to a distance of  $3 r_{\text{vir}}$ . Notably, a successful physical model should also account for the observed Ly $\alpha$  surface brightness profile that shows a power-law decrease within 20kpc and a tentative flat trend at 30 – 50 kpc (paper I).

#### 4.1. Outflows and inflows

The Ly $\alpha$  line in most LAEs is observed to be redshifted relative to  $z_{\text{sys}}$ . This is commonly attributed to the back-scattering of expanding gas flows (e.g. Dijkstra et al. 2006a; Dijkstra & Kramer 2012; Verhamme et al. 2006). Models of Ly $\alpha$  photons scattering from a central source into an outflowing medium have successfully reproduced the observed redshifted and redskewed Ly $\alpha$  line profiles (e.g. Hashimoto et al. 2015; Chang et al. 2023). In our stacked spectra (top panels in Figure 3), we also observe a red-asymmetric Ly $\alpha$  line with a redshift of approximately 170 km/s relative to  $z_{\text{sys}}$ .

Not many idealized models engage in explaining the spatially-resolved features of LAHs. To account for the observed large-scale blueshift of the Ly $\alpha$  line out to 60kpc, one possibility is a gradually decelerating outflow (e.g. Song et al. 2020, Garel et al. in preparation). The decelerating outflow could produce Ly $\alpha$  line with a smaller velocity offset, but it cannot be smaller than  $z_{\text{sys}}$ . These scattering models inherently predict a monotonically decreasing Ly $\alpha$  surface brightness profile, which is at odds with our observations presented in Paper I.

The work of Blaizot et al. (2023) suggests an alternative scenario where the strongest resonant scattering effects (broadening and redshifting of the line) happen in the inner CGM where gas densities are high. Instead, the more extended CGM (between 0.2 and  $3 r_{\text{vir}}$ ) is often dominated in volume by a hot and highly ionised outflow, which acts as a screen that intercepts blue Ly $\alpha$  photons from the galaxy and re-emits them more or less isotropically. This scattering process in the outer CGM will produce an increasingly blue profile moving away from the central source. This scenario, which we are testing (Guo et al. in preparation) is at least qualitatively consistent with our observation.

An alternative perspective considers the role of inflows. Chung et al. (2019) simulate a LAH around a galaxy with a stellar mass of  $10^{10.5} M_{\odot}$  and suggest that galactic outflows primarily affect the Ly $\alpha$  properties within  $\approx 50$  kpc, while cold accretion flows are dominant at larger radii. Based on the observation of an enormous Ly $\alpha$  blob, Li et al. (2022) provide a model in which the Ly $\alpha$  photons are produced by star formation in the galaxy and propagate outwards within multiphase clumpy outflows. Near the blob outskirts, infalling cool gas shapes the observed blue-dominated Ly $\alpha$  line, albeit with a very low contribution to the total Ly $\alpha$  luminosity. This combination of outflows and inflows is also inferred from H I absorption by Chen et al. (2020). They observe an asymmetry of Ly $\alpha$  absorption line, and explain it as infilling by blueshifted Ly $\alpha$  emission relative to  $z_{\text{sys}}$ . They also claim a transition between outflow-dominated ( $r \lesssim 50$  kpc) and accretion-dominated flows ( $r \gtrsim 100$  kpc) for galaxies with  $z \approx 2.2$  and  $M_{*} \approx 10^{10} M_{\odot}$  by comparing their observations with models.

The blueshifted and blue-skewed Ly $\alpha$  line could favor a scenario in which a non-negligible fraction of Ly $\alpha$  photons is propagated in gas inflows. The Ly $\alpha$  blueshift is seen in both mean and median, suggesting that these large-scale gas inflows are a common phenomenon around LAEs. From the perspective of surface brightness, the flattening of the profile at large radii in Paper I suggests a change in the dominant power source. The power source could be cooling radiation, which converts gravi-

tational energy into kinetic and thermal energy through collision (e.g. Haiman et al. 2000; Furlanetto et al. 2005; Dijkstra et al. 2006a,b; Rosdahl & Blaizot 2012). Fluorescence may also play an important role in powering the LAHs at large radii (e.g. Gould & Weinberg 1996; Cantalupo et al. 2005; Furlanetto et al. 2005; Mas-Ribas & Dijkstra 2016; Gallego et al. 2018, 2021). Considering Ly $\alpha$  photons produced by fluorescence subsequently scatter in the CGM, inflows and outflows would produce blue- and red-skewed Ly $\alpha$  lines, respectively.

The “outflows + inflows” model seems to offer a plausible explanation for the observed Ly $\alpha$  kinematics. Outflows can produce the redshifted Ly $\alpha$  line in the central galaxy. With increasing distance, inflows may be responsible for the observed blueshift trend. Better models and simulations are necessary to understand both the powering sources and kinematic behaviors of LAHs. To further investigate this, we conduct detailed simulations as will be described in Guo et al. in preparation.

#### 4.2. Other possibilities

Neighboring galaxies could also contribute to the observed characteristics of LAHs, whether they are satellite galaxies (e.g. Momose et al. 2016; Mas-Ribas et al. 2017; Mitchell et al. 2021) or more massive systems (e.g. Byrohl et al. 2021). The Ly $\alpha$  emission from the neighboring galaxies should, on average, be redshifted relative to  $z_{\text{sys}}$  due to radiative transfer effects. However, satellites with lower star-formation rates could potentially drive weaker winds, leading to smaller velocity offsets (Muzahid et al. 2020).

### 5. Summary

The main focus of this paper is to report the discovery of a large-scale blueshift of diffuse Ly $\alpha$  emission (with respect to the central Ly $\alpha$  red peak) out to large radii. Such a spatially-resolved weak signal can only be detected by efficient IFU facilities such as MUSE, and with ultra deep exposures such as the MXDF survey. The main results are summarized as follows:

From the galaxy out to  $\approx 60$  kpc, we detect a 250 km/s blueshift of Ly $\alpha$  emission line with respect to the Ly $\alpha$  red peak of the target LAE. However, we cannot determine if the Ly $\alpha$  line at the large distance is bluer than  $z_{\text{sys}}$ . This trend is observed in both the mean and median stacks, and is thus ubiquitous among LAEs at  $3 < z < 4$  with  $L_{\text{Ly}\alpha} = 10^{41.1} \text{ erg s}^{-1}$ .

We discuss the possible mechanisms to explain the blueshift of Ly $\alpha$  emission. Our observation favors a scenario in which the inner part of the LAH is dominated by resonant-scattered Ly $\alpha$  photons from the outflowing gas, while the dominance of inflows gradually increases out to  $\approx 60$  kpc. However, we cannot rule out the contribution from other scenarios, such as satellites.

Obviously, this work is limited by the absence of  $z_{\text{sys}}$ . The key to tackling this problem is to obtain the rest-frame optical spectra. In addition, high spectral resolution IFU facilities (e.g., BlueMUSE, Richard et al. 2019) are needed for precisely measuring the velocity shift. Spatially- and spectrally-resolved analytical models and simulations are also needed for better interpretation of the observational data (e.g. Blaizot et al. 2023).

*Acknowledgements.* Y.G., R.B. acknowledge support from the ANR L-INTENSE (ANR-20-CE92-0015). L.W. acknowledges support by the ERC Advanced Grant SPECIMAG-CGM (GA101020943). J.Brinchmann acknowledges support by Fundação para a Ciência e a Tecnologia (FCT) through the research grants UID/FIS/04434/2019, UIDB/04434/2020, UIDP/04434/2020 and

PTDC/FIS-AST/4862/2020. J.Brinchmann acknowledges support from FCT work contract 2020.03379.CEECIND.

## References

- Bacon, R., Brinchmann, J., Conseil, S., et al. 2023, A&A, 670, A4  
 Bacon, R., Mary, D., Garel, T., et al. 2021, A&A, 647, A107  
 Blaizot, J., Garel, T., Verhamme, A., et al. 2023, MNRAS, 523, 3749  
 Byrohl, C., Nelson, D., Behrens, C., et al. 2021, MNRAS, 506, 5129  
 Cantalupo, S., Porciani, C., Lilly, S. J., & Miniati, F. 2005, ApJ, 628, 61  
 Chang, S.-J., Yang, Y., Seon, K.-I., Zabludoff, A., & Lee, H.-W. 2023, ApJ, 945, 100  
 Chen, Y., Steidel, C. C., Hummels, C. B., et al. 2020, MNRAS, 499, 1721  
 Chung, A. S., Dijkstra, M., Ciardi, B., Kakiichi, K., & Naab, T. 2019, MNRAS, 484, 2420  
 Claeysens, A., Richard, J., Blaizot, J., et al. 2019, MNRAS, 489, 5022  
 Dijkstra, M., Haiman, Z., & Spaans, M. 2006a, ApJ, 649, 14  
 Dijkstra, M., Haiman, Z., & Spaans, M. 2006b, ApJ, 649, 37  
 Dijkstra, M. & Kramer, R. 2012, MNRAS, 424, 1672  
 Erb, D. K., Li, Z., Steidel, C. C., et al. 2023, ApJ, 953, 118  
 Erb, D. K., Steidel, C. C., & Chen, Y. 2018, ApJ, 862, L10  
 Furlanetto, S. R., Schaye, J., Springel, V., & Hernquist, L. 2005, ApJ, 622, 7  
 Gallego, S. G., Cantalupo, S., Lilly, S., et al. 2018, MNRAS, 475, 3854  
 Gallego, S. G., Cantalupo, S., Sarpas, S., et al. 2021, MNRAS, 504, 16  
 Garel, T., Blaizot, J., Guiderdoni, B., et al. 2015, MNRAS, 450, 1279  
 Gould, A. & Weinberg, D. H. 1996, ApJ, 468, 462  
 Guo, Y., Bacon, R., Wisotzki, L., et al. 2023, arXiv:2309.05513  
 Guo, Y., Jiang, L., Egami, E., et al. 2020, ApJ, 902, 137  
 Haiman, Z., Spaans, M., & Quataert, E. 2000, ApJ, 537, L5  
 Hashimoto, T., Verhamme, A., Ouchi, M., et al. 2015, ApJ, 812, 157  
 Kikuchi, S., Harikane, Y., Ouchi, M., et al. 2022, ApJ, 931, 97  
 Kikuta, S., Ouchi, M., Shibuya, T., et al. 2023, arXiv e-prints, arXiv:2305.08921  
 Kusakabe, H., Verhamme, A., Blaizot, J., et al. 2022, A&A, 660, A44  
 Leclercq, F., Bacon, R., Verhamme, A., et al. 2020, A&A, 635, A82  
 Leclercq, F., Bacon, R., Wisotzki, L., et al. 2017, A&A, 608, A8  
 Li, Z., Steidel, C. C., Gronke, M., Chen, Y., & Matsuda, Y. 2022, MNRAS, 513, 3414  
 Lujan Niemeyer, M., Komatsu, E., Byrohl, C., et al. 2022, ApJ, 929, 90  
 Mas-Ribas, L. & Dijkstra, M. 2016, ApJ, 822, 84  
 Mas-Ribas, L., Dijkstra, M., Hennawi, J. F., et al. 2017, ApJ, 841, 19  
 McLinden, E. M., Finkelstein, S. L., Rhoads, J. E., et al. 2011, ApJ, 730, 136  
 Mentuch Cooper, E., Gebhardt, K., Davis, D., et al. 2023, ApJ, 943, 177  
 Mitchell, P. D., Blaizot, J., Cadiou, C., et al. 2021, MNRAS, 501, 5757  
 Momose, R., Ouchi, M., Nakajima, K., et al. 2014, MNRAS, 442, 110  
 Momose, R., Ouchi, M., Nakajima, K., et al. 2016, MNRAS, 457, 2318  
 Muzahid, S., Schaye, J., Marino, R. A., et al. 2020, MNRAS, 496, 1013  
 Ono, Y., Itoh, R., Shibuya, T., et al. 2021, ApJ, 911, 78  
 Ouchi, M., Ono, Y., & Shibuya, T. 2020, ARA&A, 58, 617  
 Ouchi, M., Shimasaku, K., Akiyama, M., et al. 2008, ApJS, 176, 301  
 Richard, J., Bacon, R., Blaizot, J., et al. 2019, arXiv e-prints, arXiv:1906.01657  
 Richard, J., Claeysens, A., Lagattuta, D., et al. 2021, A&A, 646, A83  
 Rosdahl, J. & Blaizot, J. 2012, MNRAS, 423, 344  
 Shibuya, T., Kashikawa, N., Ota, K., et al. 2012, ApJ, 752, 114  
 Shibuya, T., Ouchi, M., Nakajima, K., et al. 2014, ApJ, 788, 74  
 Song, H., Seon, K.-I., & Hwang, H. S. 2020, ApJ, 901, 41  
 Steidel, C. C., Bogosavljević, M., Shapley, A. E., et al. 2011, ApJ, 736, 160  
 Verhamme, A., Garel, T., Ventou, E., et al. 2018, MNRAS, 478, L60  
 Verhamme, A., Schaerer, D., & Maselli, A. 2006, A&A, 460, 397  
 Wisotzki, L., Bacon, R., Blaizot, J., et al. 2016, A&A, 587, A98  
 Wisotzki, L., Bacon, R., Brinchmann, J., et al. 2018, Nature, 562, 229